





Article

Reducing the Transition Hysteresis of Inductive Plasmas by a Microwave Ignition Aid

Tim Gehring ^{*}, Qihao Jin , Fabian Denk, Santiago Eizaguirre, David Karcher and Rainer Kling

Light Technology Institute, Karlsruhe Institute of Technology, Engesserstr. 13, 76131 Karlsruhe, Germany

^{*} Correspondence: tim.gehring@kit.edu

Received: 25 June 2019; Accepted: 9 August 2019; Published: 16 August 2019



Abstract: Inductive plasma discharge has been a part of continuous investigations since it was discovered. Especially the E- to H-mode transition and the hysteresis behavior have been topics of research in the last few decades. In this paper, we demonstrate a way to reduce the hysteresis behavior by the usage of a microwave ignition system. With this system, a significant decrease of the needed coil current for the ignition of the inductive driven plasma is realized. For the microwave generation, a magnetron as in a conventional microwave oven is used, which offers a relatively inexpensive way for microwave ignition aid. At the measured pressure of 7.5 Pa, it was possible to reduce the needed coil current for the inductive mode transition by a factor of 3.75 compared to the mode transition current without the ignition aid. This was achieved by initiating the transition by a few seconds of microwave coupling. The performed simulations suggested that the factor can be further increased at higher pressures. That is especially interesting for plasmas that are hard to ignite or for RF-sources that cannot deliver high enough currents or frequencies for the ignition.

Keywords: inductive plasma; ICP; mode transition; plasma ignition; microwave; ignition aid

1. Introduction

Inductively-coupled plasmas (ICPs) are applied in a wide range of areas, from surface treatment to lighting applications. Since wide bandgap transistors made of semiconductor materials like SiC and GaN are available, it is possible to build highly-efficient inverters for a frequency up to 3 MHz [1]. Compared to the commonly-used frequency of 13.56 MHz, the needed coil currents for the ignition of 3-MHz-driven plasmas are drastically higher. In addition, the size of the coil used and the material that has to be ionized for the discharge are parameters with a large influence on the ignition current [2–4]. Therefore, the ignition behavior of this kind of plasma is investigated. A conventional magnetron was used for an additional power coupling to reduce the hysteresis behavior during the E- to H-mode transition. The results showed that due to the microwave ignition aid, the high frequency power source needs to deliver only the minimum maintenance current for the plasma ignition at a defined pressure.

The basis for the investigations was the model for the minimum ignition field according to Burm [2] and the analytical estimation of the minimum maintenance current according to Kortshagen [5]. The minimum ignition field approach is a relationship of the magnetic breakdown to the Paschen law. Usually, the Paschen law and the breakthrough condition are not used to describe the ICP ignition [6]. However, the theory can be justified by the results in Section 3. The chosen approach describes the minimum magnetic breakdown field B_{ign} as:

$$B_{\text{ign}} = \frac{B_0 p}{\omega R [\ln(A_0 \pi p R) - \ln(\ln(\frac{\gamma+1}{\gamma}))]} \quad (1)$$

where A_0 and B_0 are the Paschen parameters, which can also be used for inductive operation. The excitation frequency used is given by the angular frequency ω and the pressure p . The radius of the coil corresponds to R . Here, the radius of the plasma vessels r was chosen as nearly $r \approx R$. The secondary electron emission coefficient γ originally described the generation rate of the secondary electrons at the electrodes [7]. Since there are no electrodes for inductive excitation, this value was set to $\gamma = \frac{1}{e-1}$ to neglect the negative double-logarithmic term for the first approximation. A detailed derivation can be found in [2]. The calculated minimum ignition field B_{ign} for the configuration used is shown in Figure 1.

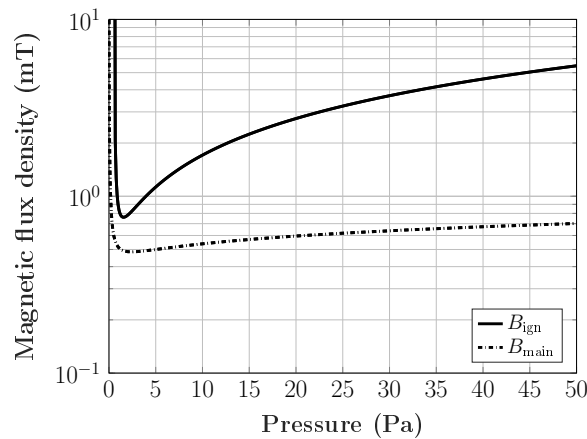


Figure 1. Ignition field B_{ign} and maintenance field B_{main} over the pressure calculated for Xenon in a $r = 28.5$ -mm vessel.

The minimum maintenance current was approximated numerically. According to Kortshagen [5], with the known geometry and impedance Z of the system, the minimum maintenance current I_{min} can be determined by calculating the electric field E_0 along the coil as:

$$I_{min} = \frac{2LM}{|Z|} 2\pi R E_0 \tag{2}$$

where L corresponds to half of the coil length and M to the winding density. For the calculation of the field E_0 , the Finite Element Method (FEM) software COMSOLTM (COMSOL AB, Stockholm, Sweden) was used [8]. This software includes a module for ICP simulations. In this article only the most important formulas used from the software to simulate the plasma parameters will be introduced. An exact overview of the main simulation theory can be found in [9]. The simulation was performed as a sweep over the pressure. The pressure dependence of the plasma parameters was then taken into account by the software. To estimate the minimum maintenance current I_{min} , a set of plasma parameters is needed. To create this set, an external power has to be applied in the simulation. Therefore, the presented simulation yielded a solution that was not explicit. However, we found that if the minimum ignition current derived from B_{ign} from Equation (1) was the base for the parameter calculation, the results delivered a good first step approximation for I_{min} . To calculate the plasma properties, the following equations are solved:

$$\frac{\partial n_e}{\partial t} + \nabla \cdot \Gamma_e = R_e - (u \cdot \nabla) n_e \tag{3}$$

$$\Gamma_e = -(\mu_e E) n_e - \nabla (D_e N_e)$$

$$\frac{\partial n_e}{\partial t} + \nabla \cdot \Gamma_e + E \cdot \Gamma_e = S_{en} - (u \cdot \nabla) n_e + (Q + Q_{gen})/q \tag{4}$$

$$\Gamma_e = -(\mu_e E) n_e - \nabla (D_e N_e)$$

Equation (3) is used to calculate the time-dependent change of the electron density, where n_e is the electron density, R_e the rate of electron generation, μ_e the electron mobility, E the electric field, D_e the diffusion coefficient, and u represents the velocity vector of the neutral fluid (here Xenon). Equation (4) indicates the density of the electron energy. The symbols n_e , μ_e and D_e are given analogously to Equation (3) for the energy density. Q and Q_{gen} are given by an external and a general heat source. In addition, q is given as the charge, and S_{en} indicates the energy change by inelastic collisions. In our simulation, the reactions in Table 1 were used. For both equations, the flux terms Γ_e and Γ_ϵ are directly given. To calculate the generation rate R_e of electrons due to collisions and reactions, the cross-sections of the different Xenon species can be imported into the software. The elastic collision data from [10] and the excitation and ionization data from [11] were used.

Table 1. The processes used in the Xenon discharge for the simulation.

No.	Process	Reaction	$\Delta\epsilon$ (eV)
1	Elastic	$Xe + e \rightarrow Xe + e$	
2	Excitation	$Xe + e \rightarrow Xe^* + e$	8.31
3	Superelastic collision	$Xe^* + e \rightarrow Xe + e$	-8.31
4	Ionization	$Xe + e \rightarrow Xe^+ + 2e$	12.1
5	Step-wise ionization	$Xe^* + e \rightarrow Xe^+ + 2e$	3.8

The electromagnetic field is calculated through Ampere’s law, expressed as a function of the magnetic vector potential A , given as:

$$(j\omega\sigma - \omega^2\epsilon)A + \nabla \times (\mu_0^{-1}\nabla \times A) = J_e \tag{5}$$

where j is the imaginary unit, ϵ the permittivity, μ_0 the vacuum permeability, and J_e the external applied current density. The plasma conductivity σ is calculated by:

$$\sigma = \frac{n_e e_0^2}{m_e(v_m + j\omega)} \tag{6}$$

where e_0 represents the electron charge, m_e the electron mass, and v_m the momentum transfer frequency. Since a high-frequency sinusoidal excitation is used, a rapidly-changing magnetic field is induced in the coil. Following Faraday’s law, an electrical field dependent on the magnetic vector potential is induced:

$$E = -j\omega A \tag{7}$$

E_0 in Equation (2) is defined as the electrical field strength E at the location R . We simulated E_0 over the pressure and calculated the minimum magnetic maintenance field B_{main} by the use of I_{min} and the given coil configuration (see Section 2) as:

$$B_{main} = \mu_r \mu_0 M I_{min} \tag{8}$$

The calculated ignition and maintenance fields are shown in Figure 1. The hysteresis behavior of the mode transition could be regarded as the difference of the fields.

2. Experimental Setup

Figure 2 shows a scheme of the setup used. For the high-frequency power supply, an internally-developed inverter was used, which was presented in [1]. The output impedance was adapted to the inductive load with a matching network consisting of a tunable vacuum capacitor (500–1000 pF, WVS-Technology, Meerbusch, Germany). The coil current was measured with a wideband current monitor (Pearson Electronics, Palo Alto, CA, USA) directly at the coil input. The power output of the inverter, as well as the coil current were continuously monitored and recorded by an oscilloscope.

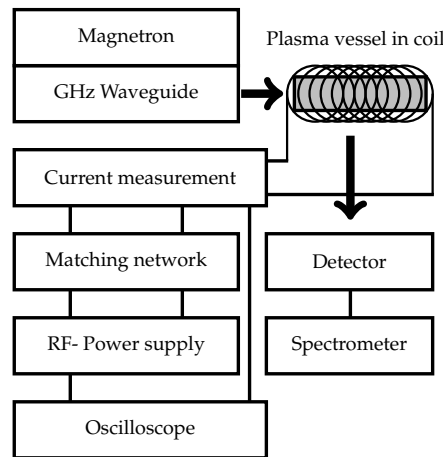


Figure 2. Scheme of the setup used.

The operation took place in an air coil made of a copper tube with internal water cooling and different winding densities. For the investigations of the magnetic ignition behavior, a coil with $n = 15$, $R = 30$ mm and $l = 100$ mm was used. For the experiments using the microwave ignition aid, the coil had to be adapted to $n = 26$, $R = 22.5$ mm and $l = 145$ mm.

The plasma was generated in cylindrical quartz vessels within the coil. These were baked under vacuum and then filled with Xenon. The filling pressures were varied from 2.5 Pa–40 Pa. Here, glass vessels with $l = 60$ mm and $r = 28.5$ mm were used. For the studies with the use of microwaves, a glass vessels with $l = 100$ mm and $r = 14.5$ mm was used. The adaptation of the coil and the lamp vessel in the microwave investigations had to be done because an adjustment of the load during operation should be prevented. With the smaller dimensions and thus a smaller power density, the operation even in non-ideal operating points was possible. The hysteresis investigations were radiation-based. The mode transition was recorded by an array spectrometer (CAS 140CT, Instrument Systems, Munich, Germany), and the microwave generation was realized by a 500-W, 2.45-GHz magnetron (2M213, HITACHI, Chiyoda, Japan). The microwave radiation was then directed by a waveguide directly into the glass vessel.

3. Results and Discussion

To validate Equation (1), the glass vessels with different Xenon pressures were placed in the coil. The coil current was slowly increased until the plasma mode transition occurred. The required ignition current was recorded by the oscilloscope. Since the ignition was based on statistical processes, this procedure was repeated several times for each pressure, and the mean value was built. The measurement results are shown in Figure 3.

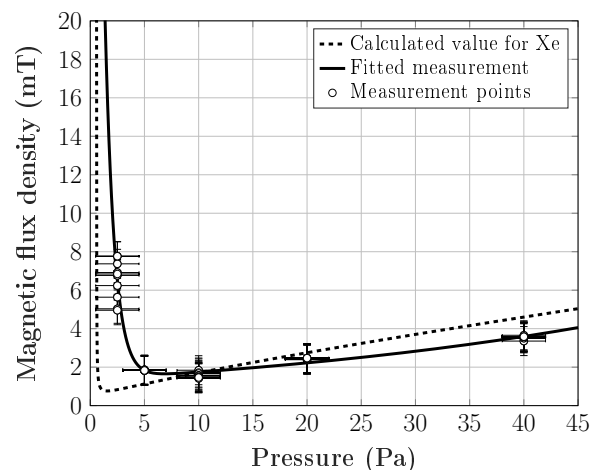


Figure 3. Calculated ignition field B_{ign} without microwave ignition aid from the current measurement for Xenon in a vessel with $r = 28.5$ mm and a coil with $R = 30$ mm, $n = 15$ over the pressure.

The measurements showed that Equation (1) gave a good approximation to the calculation of the required ignition field. The deviations in the pressure range of <5 Pa were generated by the larger statistical distribution of the ignition points. In order to produce an even more precise curve, the measurements would have to be repeated more often and at even more pressure points. Furthermore, the uncertainty of ± 2 Pa was caused by the pressure sensor and the filling station used. However, with those measurements, we found the minimum ignition field B_{ign} at a pressure of 7.5 Pa Xenon. At this point, the severe error did not influence the ignition field since the slope of the measured curve was near the minimum here. With that pressure, a lamp for the hysteresis investigation was built. For the measurement in the first step, the normal ignition behavior was observed, as shown in Figure 4 (dashed line). Therefore, the coil current was increased stepwise, and the radiation output was detected. Without the microwave ignition aid, a common transition behavior was measured. That behavior is well known and often reported [5,12,13]. For the microwave ignition study, the coil current was increased stepwise, and the microwaves were coupled into the lamp vessel. Due to the additional power, the inductive discharge ignited even at low coil currents. In that case, the additional radiation output was not relevant and so is neglected in Figure 4. Without the additional power from the microwaves, the discharge at low coil currents fell back into E-mode. After the minimum maintenance current I_{min} was exceeded, the inductive discharge stayed on (Figure 4, dotted line). The jump in the coil current was caused by the sudden decay in the impedance and was observed in both of the two ignition situations. The results showed that with the additional power from the microwaves, the needed E- to H-transition current was lowered to the minimal maintenance coil current I_{min} . Therefore, if the setup were matched to the H-mode plasma impedance, the generated high-frequency coil current would be reduced to the minimum maintenance current I_{min} . In that situation, also the E- to H-mode hysteresis was avoided. The lower transition point, which was reached with the microwave ignition aid, could be explained by the jump in the electron density during the additional power coupling. The power that could be absorbed by the plasma was proportional to the electron density [12]. If the power were increasing, a cut-off density would be reached. At this point, the capacitive power absorption was reduced while the inductive absorption was still increasing, and the E- to H-mode transition occurred [12]. In the case of a common inductive ignition, the cut-off electron density had to be reached only from the field generated by the coil. In view of the high currents, this represents a challenge to the technology, especially for hard ignitable plasmas. However, the presented pressure range has to be noted, so information on the scope of the validity of the statements made in this work is a subject of future research. In addition, investigations on the power coupling efficiencies of the microwaves have to be done to describe the power absorption more precisely.

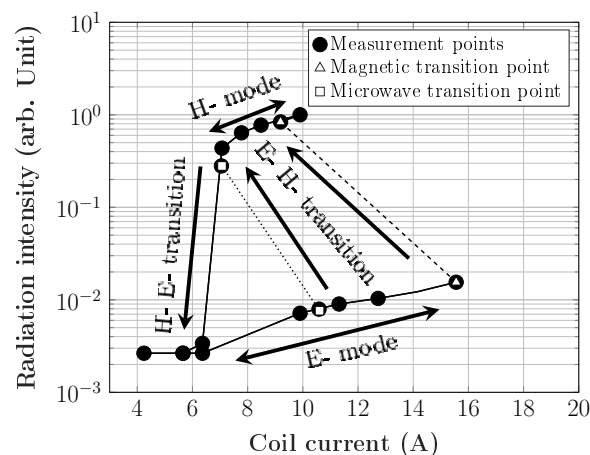


Figure 4. Hysteresis behavior with and without microwave ignition. Measured as the radiation intensity in dependence of the coil current in a $R = 22.5$ mm, $l = 145$ mm and $n = 26$ coil.

4. Conclusions

In this paper, we calculated and measured the minimum magnetic breakdown field and the minimum maintenance field for an ICP Xenon discharge. We showed that a reduction or even the prevention of the transition hysteresis seen by the coil and the high-frequency inverter can be achieved by the use of a microwave ignition aid. With this system, it is possible to reduce the needed coil current significantly, which provides a great advantage for efficient operation of the inverter used. If the inverter used is switched on during the microwave ignition, it only has to be matched to the inductive discharge impedance. This prevents a matching to the E-mode and avoids an impedance tuning during the operation. Furthermore, the usage of a common 2.45-GHz magnetron is an inexpensive and simple way to realize an ignition aid for ICPs.

Author Contributions: Conceptualization, all; methodology, all; validation, all; formal analysis, all; investigation, all; data curation, T.G.; writing—original draft preparation, T.G.; writing—review and editing, all; visualization, T.G.; supervision, R.K.; project administration, R.K.; funding acquisition, R.K.

Funding: This research was funded in part by the European Union’s Horizon 2020 research and innovation program under Grant Number 641702.

Conflicts of Interest: The authors declare no conflict of interest.

References

- Denk, F.; Haehre, K.; Simon, C.; Eizaguirre, S.; Heidinger, M.; Kling, R.; Heering, W. 25 kW high power resonant inverter operating at 2.5 MHz based on SiC SMD phase-leg modules. In Proceedings of the PCIM Europe 2018; International Exhibition and Conference for Power Electronics, Intelligent Motion, Renewable Energy and Energy Management, Nuernberg, Germany, 5–7 June 2018.
- Burm, K. Breakdown magnetic field in an inductively coupled plasma. *Phys. Lett. A* **2008**, *372*, 6280–6283. [[CrossRef](#)]
- BURM, K.T.A.L. Breakdown minimum in magnetic field-driven metal plasmas. *J. Plasma Phys.* **2011**, *77*, 675–678. [[CrossRef](#)]
- BURM, K.T.A.L. Paschen curves for metal plasmas. *J. Plasma Phys.* **2012**, *78*, 199–202. [[CrossRef](#)]
- Kortshagen, U.; Gibson, N.D.; Lawler, J.E. On the E–H mode transition in RF inductive discharges. *J. Phys. D Appl. Phys.* **1996**, *29*, 1224–1236. [[CrossRef](#)]
- BURM, K.T.A.L. The electronic identity of inductive and capacitive plasmas. *J. Plasma Phys.* **2008**, *74*, 155–161. [[CrossRef](#)]
- Lieberman, M.A.; Lichtenberg, A.J. *Principles of Plasma Discharges and Materials Processing*, 2nd ed.; Wiley-Interscience: Hoboken, NJ, USA, 2005. [[CrossRef](#)]

8. COMSOL. *Multiphysics V. 5.4*; COMSOL AB: Stockholm, Sweden. Available online: www.comsol.com (accessed on 25 June 2019).
9. COMSOL. *Plasma Module User's Guide*; COMSOL AB: Stockholm, Sweden, 2019. Available online: <https://www.doc.comsol.com/5.4/doc/com.comsol.help.plasma/PlasmaModuleUsersGuide.pdf> (accessed on 25 June 2019).
10. SIGLO Database. Available online: www.lxcat.net (accessed on 25 April 2019).
11. TRINITY Database. Available online: www.lxcat.net (accessed on 25 April 2019).
12. Lee, M.H.; Chung, C.W. On the E to H and H to E transition mechanisms in inductively coupled plasma. *Phys. Plasmas* **2006**, *13*, 063510. [[CrossRef](#)]
13. Turner, M.M.; Lieberman, M.A. Hysteresis and the E-to-H transition in radiofrequency inductive discharges. *Plasma Sources Sci. Technol.* **1999**, *8*, 313–324. [[CrossRef](#)]



© 2019 by the authors. Licensee MDPI, Basel, Switzerland. This article is an open access article distributed under the terms and conditions of the Creative Commons Attribution (CC BY) license (<http://creativecommons.org/licenses/by/4.0/>).